

93-365



Объединенный
Институт
Ядерных
Исследований
Дубна

E4-93-365

V.A.Kuz'min, A.A.Ovchinnikova, T.V.Tetereva

MUON CAPTURE BY $^{10,11}\text{B}$ NUCLEI:
SENSIBILITY TO THE NUCLEAR MODEL CHOICE

Submitted to «Ядерная физика»

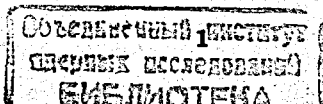
1993

1. It is well known that the characteristics of muon capture by nuclei (ordinary and radiative) are sensitive to the parameters of a weak hadron current and, specifically, to a value of a pseudoscalar coupling constant g_p . The analysis of first data on a radiative muon capture by a hydrogen [1] has shown that the value of g_p is slightly greater than the values defined from the Goldberger-Treiman relation. Investigation of partial transitions in μ -capture on more complex nuclei would make it possible to determine the value of g_p as well and thus to verify the validity of the Goldberger-Treiman relation in nuclei.

In the last time the process of muon capture by atomic nuclei receives much interest because the modern experimental technique allows one to determine the characteristics of this process with rather a high accuracy. The general theory of muon capture by atomic nuclei has been developed rather long ago [2, 3]. However, a theoretical analysis of this process was always hindered by uncertainties caused by the choice of a model for describing the atomic nucleus. In connection with experimental investigations planned at PSI (Switzerland) [4], the analysis of this reaction on the basis of the current notions about the atomic nucleus structure seems to be timely. The aim of a similar analysis should be estimation of uncertainty on the predicted characteristics of the process caused by the choice of a model to describe nuclear wave functions. In the present paper, we consider the sensitivity of the capture rate of a muon being in a certain state of the hyperfine structure of mesic atoms in $^{10,11}B$ to the choice of nuclear wave functions. These nuclei are used as targets in the experiment that is conducted now by PSI and Universite Catholique de Louvain, Belgium groups. The Laboratory of Nuclear Problems of JINR participates in this experiment too.

2. The rate of the ordinary muon capture (OMC) from the hyperfine state with spin \mathcal{F} of a mesic atom is determined for the general case by the formulae

$$\Lambda^{\mathcal{F}^+} = V \frac{1}{2(I_i + 1)} \sum_{J=0}^{J_{\max}} \frac{1}{J+1} \cdot \\ \left\{ \left[\sqrt{(I_f + I_i + 2 + J)(I_i - I_f + 1 + J)} M_J(J+1) - \right. \right. \\ \left. \left. - \sqrt{(I_f - I_i + 1 + J)(I_f + I_i - J)} M_{J+1}(J+1) \right]^2 + \right.$$



$$+[\sqrt{(I_f+I_i+2+J)(I_i-I_f+1+J)}M_J(-J-1) - \sqrt{(I_f-I_i+1+J)(I_f+I_i-J)}M_{J+1}(-J-1)]^2\}, \quad (1)$$

$$\Lambda^{\mathcal{F}^-} = V \frac{1}{2I_i} \sum_{J=0}^{J_{max}} \frac{1}{J+1} \{[\sqrt{(I_f+I_i+2+J)(I_i-I_f+1+J)}M_{J+1}(J+1) + \sqrt{(I_f-I_i+1+J)(I_f+I_i-J)}M_J(J+1)]^2 + [\sqrt{(I_f+I_i+2+J)(I_i-I_f+1+J)}M_{J+1}(-J-1) + \sqrt{(I_f-I_i+1+J)(I_f+I_i-J)}M_J(-J-1)]^2\}, \quad (2)$$

$$V = \frac{2I_f+1}{2I_i+1} [G \cos \Theta_c m_\mu^2 \frac{m_\mu}{\hbar} 4 [\frac{\alpha Z}{1+\frac{m_\mu}{AM_N}}]^3 R_\mu(Z) (\frac{E_\nu}{m_\mu})^2 (1 - \frac{E_\nu}{m_\mu + M_i})],$$

$$\mathcal{F}^+ = I_i + \frac{1}{2}, \quad \mathcal{F}^- = I_i - \frac{1}{2}, \quad J_{min} = |I_i - I_f|, \quad J_{max} = I_i + I_f,$$

here I_i and I_f are spins of the initial and final states of the nucleus. At statistical population of levels of the hyperfine structure, the total OMC rate is

$$\Lambda^{stat} = V \frac{2I_f+1}{2I_i+1} \sum_{J=J_{min}}^{J_{max}} \{M_J^2(-J-1) + M_J^2(J) + M_J^2(J+1) + M_J^2(-J)\}. \quad (3)$$

Here, we use the notation introduced in paper [3] (formulae(3.20)). Independent amplitudes $M_J(\kappa)$ describe the transition at which the total momentum J is transferred to the nucleus and the created neutrino state is characterized by the quantum number κ ; κ is the eigenvalue of the operator $-(\vec{l}, \vec{\sigma}) - 1$. It was assumed in deriving formulae (1)-(3) that the muon is a nonrelativistic particle that was captured from the lowest s -state; $R_\mu(Z)$ is the proportionality coefficient between the square of the mean absolute value of the muon function inside the nucleus and the square of the absolute value of the muon wave function in the field of the pointlike charge Ze at $\vec{r} = 0$; $R_\mu = 0.849$ for $^{10,11}B$

[5]. It should be mentioned that formulae (1)-(2) differ from those of [3]. The interference between the transitions of different forbiddenness order is taken into account more accurately in the formulae presented here.

For the partial transitions considered

$$\mu^- + {}^{10}B(3g.s.) \rightarrow \nu + {}^{10}Be(2_{1,2}^+), \quad (4)$$

$$\mu^- + {}^{11}B((3/2)g.s.) \rightarrow \nu + {}^{11}Be((1/2)_1^-) \quad (5)$$

formulae (1)-(2) can be written as

$$\Lambda^{\mathcal{F}^+} = \frac{V}{2(I_i+1)} \{[\sqrt{(I_f+I_i+2)(I_i-I_f+1)}M_0(-1) - \sqrt{(I_f-I_i+1)(I_f+I_i)}M_1(-1)]^2 + \frac{1}{2}[\sqrt{(I_f+I_i+3)(I_i-I_f+2)}M_1(2) - \sqrt{(I_f-I_i+3)(I_f+I_i-1)}M_2(2)]^2 + \frac{1}{3}[\sqrt{(I_f+I_i+4)(I_i-I_f+3)}M_2(-3) - \sqrt{(I_f-I_i+4)(I_f+I_i-2)}M_3(-3)]^2 + \frac{1}{4}[\sqrt{(I_f+I_i+5)(I_i-I_f+4)}M_3(4) - \sqrt{(I_f-I_i+5)(I_f+I_i-3)}M_4(4)]^2\}, \quad (6)$$

$$\Lambda^{\mathcal{F}^-} = \frac{V}{2(I_i+1)} \{[\sqrt{(I_f+I_i+2)(I_i-I_f+1)}M_1(-1) + \sqrt{(I_f-I_i+1)(I_f+I_i)}M_0(-1)]^2 + \frac{1}{2}[\sqrt{(I_f+I_i+3)(I_i-I_f+2)}M_2(2) + \sqrt{(I_f-I_i+3)(I_f+I_i-1)}M_1(2)]^2 + \frac{1}{3}[\sqrt{(I_f+I_i+4)(I_i-I_f+3)}M_3(-3) + \sqrt{(I_f-I_i+4)(I_f+I_i-2)}M_4(-3)]^2\}$$

$$\begin{aligned}
& + \sqrt{(I_f - I_i + 4)(I_f + I_i - 2)M_2(-3)}^2 + \\
& + \frac{1}{4} \left[\sqrt{(I_f + I_i + 5)(I_i - I_f + 4)M_4(4)} + \right. \\
& \left. + \sqrt{(I_f - I_i + 5)(I_f + I_i - 3)M_3(4)}^2 \right] \quad (7)
\end{aligned}$$

and coincide with formulae (2)–(3) of [6].

The main contribution to the rates of transitions considered comes from the amplitudes of the so-called allowed transitions, $M_1(-1)$ and $M_1(2)$, which determine the dependence of Λ^+ and Λ^- on g_p .

$$\begin{aligned}
M_1(-1) = & \sqrt{\frac{2}{3}} \left\{ -\left(G_A - \frac{1}{3}G_p\right)[101] - \right. \\
& \left. -G_p \frac{\sqrt{2}}{3}[121] - \frac{g_A}{M}[011p] + \frac{g_v}{M} \sqrt{\frac{2}{3}}[111p] \right\}, \quad (8)
\end{aligned}$$

$$\begin{aligned}
M_1(2) = & \sqrt{\frac{2}{3}} \left\{ -G_p \frac{\sqrt{2}}{3}[101] - \right. \\
& \left. -\left(G_A - \frac{2}{3}G_p\right)[121] + \frac{g_A}{M}\sqrt{2}[011p] + \frac{g_v}{M}\sqrt{\frac{1}{3}}[111p] \right\}, \quad (9)
\end{aligned}$$

here G_i are the standard combinations of the weak form factors, $[..J]$ are the nuclear matrix elements, (for definitions see [3]). Among them $[101]$ describes the Gamow-Teller transition and $[..p]$ are so-called velocity dependent terms. If the Gamow-Teller matrix element is much greater than all other nuclear matrix elements, the rate Λ^+ that will be proportional to $G_p^2[101]^2$, turns out to be very sensitive to the value of g_p . The g_p -dependence of the rate Λ^- , that will be proportional to the $(G_A - G_p/3)^2[101]^2$, is more weak. In this case, the ratio Λ^+/Λ^- , which is of greater interest from the experimental point of view, turns out to be sensitive to the value of g_p and simultaneously, free from uncertainties connected with the nuclear structure. However, the values of the velocity matrix elements are usually close to the Gamow-Teller ones. If, in the general case, the contribution of the velocity dependent matrix elements to the amplitude $M_1(-1)$ amounts to 10 per cent, then to the amplitude $M_1(2)$ and consequently to Λ^+ it is more than 20 per cent. The amplitude $M_1(2)$ is as a rule smaller than $M_1(-1)$ and can be compared in value with the second forbiddenness amplitudes. So, when one calculates Λ^+ , it is essential to take into account the contribution of $M_J(\kappa)$ for all possible J and κ .

3. Shell models are most convenient for describing the structure of light nuclei. In these models the space of single-particle states occupied by valence nucleons, energies of these states and two-particle interactions between valence nucleons are determined. The shell model for nuclei of the $0p$ shell is well known [7]. In our calculations along with the classical three versions of the shell model of the above-mentioned paper we also use three sets of single-particle energies and two-particle interactions of ref.[8]. By different nuclear models, we will speak about, we mean shell models with different sets of single-particle energies and two-matrix elements, i.e., different sets of parameters of the shell model Hamiltonian. For the ^{10}B and ^{10}Be states we have also made calculations in the shell space containing the $0p$, $1s$ and $0d$ shells [9]. The notation for nuclear models we use and the relevant references are given in table 1.

As the effective Hamiltonian is taken in the impulse approximation as a sum of single-particle operators, calculation of matrix elements of the effective Hamiltonian is reduced to contraction of matrix elements $S(O^{(\Delta_J, \Delta_T)}, \alpha, \alpha')$ corresponding to transitions between single-particle states α and α' of the shell space with single-particle transition densities $A(\Delta_J, \Delta_T, \alpha, \alpha', f, i)$ [10] (formula (33) therein):

$$\langle f || O^{(\Delta_J, \Delta_T)} || i \rangle = \sum_{\alpha, \alpha'} A(\Delta_J, \Delta_T, \alpha, \alpha', f, i) S(O^{(\Delta_J, \Delta_T)}, \alpha, \alpha').$$

In fact, these transition densities are reduced matrix elements of the tensor products of the particle creation and annihilation operators on the levels α and α' between the wave functions of the initial and final nuclear states and determine single-particle amplitudes forming a transition from one many-particle state to another

$$A(\Delta_J, \Delta_T, \alpha, \alpha', f, i) = \frac{\langle f || [a^\dagger(\alpha) \otimes \bar{a}(\alpha')]^{(\Delta_J, \Delta_T)} || i \rangle}{\sqrt{(2\Delta_J + 1)(2\Delta_T + 1)}}$$

The nuclear wave functions and one-body transition densities were calculated with the aid of computer code [11]. To evaluate the single-particle integrals, the wave functions of the isotropic harmonic oscillator were used. The characteristic length of the potential wall was equal to 1.64 fm for ^{10}B , ^{10}Be and 1.65 fm for ^{11}B , ^{11}Be .

4. In the capture of muons by the nucleus ^{10}B two allowed transitions are possible to the 2_1^+ levels with an excitation energy of 3.37 MeV and

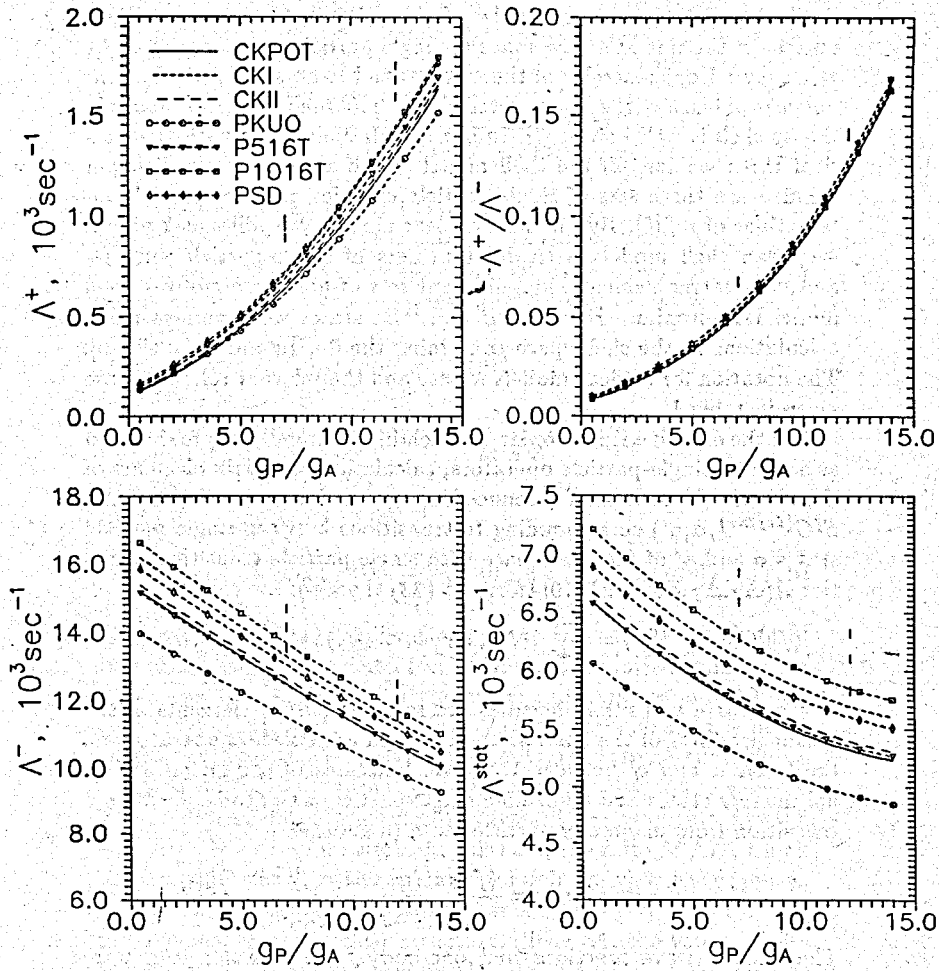


Fig. 1. Ordinary muon capture rates for partial transition $\mu^- + {}^{10}\text{B}(3_{g.s.}^+) \rightarrow \nu + {}^{10}\text{Be}(2_2^+, 5.26)$, calculated for several nuclear models. The results of [6](table IV) are denoted by vertical bars

2_2^+ with an excitation energy of 5.96 MeV. From the experimental point of view, the transition to the 2_2^+ state $\mu^- + {}^{10}\text{B}(3_{g.s.}^+) \rightarrow \nu + {}^{10}\text{Be}(2_2^+)$ is more interesting. Table 2 contains single-particle transition densities obtained for the nuclear models mentioned above. As is seen from the table, the transition amplitude for the operators of rank 1 from the $0p_{3/2}$ state to the $0p_{1/2}$ state is considerably larger than amplitudes of the other transitions. Moreover, the value of this amplitude in passing from one nuclear model to another changes by no more than 10 per cent whereas the transition densities for the other single-particle transitions may change several times. This is due to the fact that the wave functions of the ground state of ${}^{10}\text{B}$ and of the excited 2_2^+ level of ${}^{10}\text{Be}$ contain leading components whose contribution changes slightly in passing from one nuclear model to another. The behaviour like that of the transition density leads to that the independent nuclear amplitudes describing allowed transitions, $M_1(-)$ and $M_1(2)$, are considerably larger than the amplitudes forbidden by the second order and shows a weak dependence on a nuclear model. Expansion of the shell space by adding states from the $1s$ and $0d$ shell does not change essentially the structure of the wave functions ${}^{10}\text{B}(g.s.)$ and ${}^{10}\text{Be}(2_2^+)$, and consequently, the distribution of single-particle transition densities (see table 2, PSD row).

Fig. 1 shows the dependence of the capture rates Λ^+ , Λ^- , Λ^{stat} and the ratio Λ^+/Λ^- on the value of the pseudoscalar constant. As was expected, in the cases when the behaviour of velocities is determined by the amplitudes of allowed transitions, $M_1(-)$ and $M_1(2)$, the value of Λ^- weakly depends on the pseudoscalar whereas Λ^+ changes several times if g_P changes from $2g_A$ to $14g_A$. The ratio Λ^+/Λ^- turns out to be a most sensitive characteristic of the quantity g_P and is almost independent of a nuclear model though ambiguity in the choice of a nuclear model leads to a 10 per cent ambiguity in values of the velocities Λ^+ and Λ^- . Fig. 1 also shows the results obtained in ref.[6]. It is seen that these results essentially differ from ours as regards determination of the quantity Λ^+ , and which is more important, determination of Λ^+/Λ^- . This is due to the fact that in ref. [6] an anomalously large estimate of the matrix element [123]: $[123]/[121] \sim 15$ has been obtained. In all the models we use this ratio is much smaller (3÷5). The large matrix element [123] leads to that the amplitude forbidden by the second order $M_3(-3)$ is comparable with the amplitude $M_1(2)$ (see

table 3; the amplitudes of ref.[6] are cited from [12]) and noticeably changes the quantity Λ^+ . The quantity Λ^- is affected by an increase of $M_3(-3)$ to a much lesser degree since Λ^- is mainly determined by the amplitude $M_1(-1)$.

5. $\mu^- + {}^{10}\text{B}(3_{g.s.}^+) \rightarrow \nu + {}^{10}\text{Be}(2_1^+)$. For the partial transition to the ${}^{10}\text{Be}(2_1^+)$ state the picture changes drastically. The absence of the leading component in the wave function of this state leads to that the transition density is distributed over single-particle transitions more uniformly (see table 4). In this case, first rank transitions do not manifest themselves considerably among others. Transition to a new nuclear model leads to a noticeable change in the transition density. It is essential that the weight of the single-particle transition $p_{3/2} \rightarrow p_{1/2}$, which is the largest among the $J = 1$ transitions, varies several times. As a result, the amplitudes of allowed transitions, $M_1(-1)$ and $M_1(2)$, strongly depend on the choice of a nuclear model (see table 5). The amplitude $M_3(-3)$ becomes comparable in value with the amplitudes of allowed transitions. Fig. 2 exemplifies the curves of the dependence of the velocities Λ^+ , Λ^- , Λ^{stat} and the ratio Λ^+/Λ^- on the quantity g_P/g_A . In accordance with table 5, the transition rates change several times when passing from one nuclear model to another. Since for this transition the amplitudes of allowed transitions ($J = 1$) are suppressed and are not now dominating, in different models different are not only the values of the rates Λ^+ and Λ^- but also the nature of their dependence on the pseudoscalar. This is especially clearly seen on the quantity Λ^+ . Since in $M_J(-J)$ the dependence of the pseudoscalar has the form $(G_A - G_P)$ and the amplitude $M_J(J+1)$ is proportional to G_P , those models in which $M_3(-3)$ is comparable or larger than $M_1(2)$ give a weak dependence of Λ^+ on G_P . A "random" nature of changes in the transition densities in passing from one nuclear model to another results in that the ratio Λ^+/Λ^- is also less sensitive to g_P and strongly depends on the choice of a nuclear model.

Fig. 2 and table 5 show the results of calculations from ref. [6]. As with the transition to the 2_2^+ level, nuclear amplitudes of rank 1 and 2 approximately agree with ours. An increase in the amplitudes of the rank 3 is caused by a larger value [123] than ours. Thus, the amplitude $M_3(-3)$ almost three times exceeds the amplitude $M_1(-1)$. Therefore, the values of Λ^+ and Λ^- , obtained in ref. [6], are much larger than those calculated by us and cannot be placed on fig. 2. It is to be

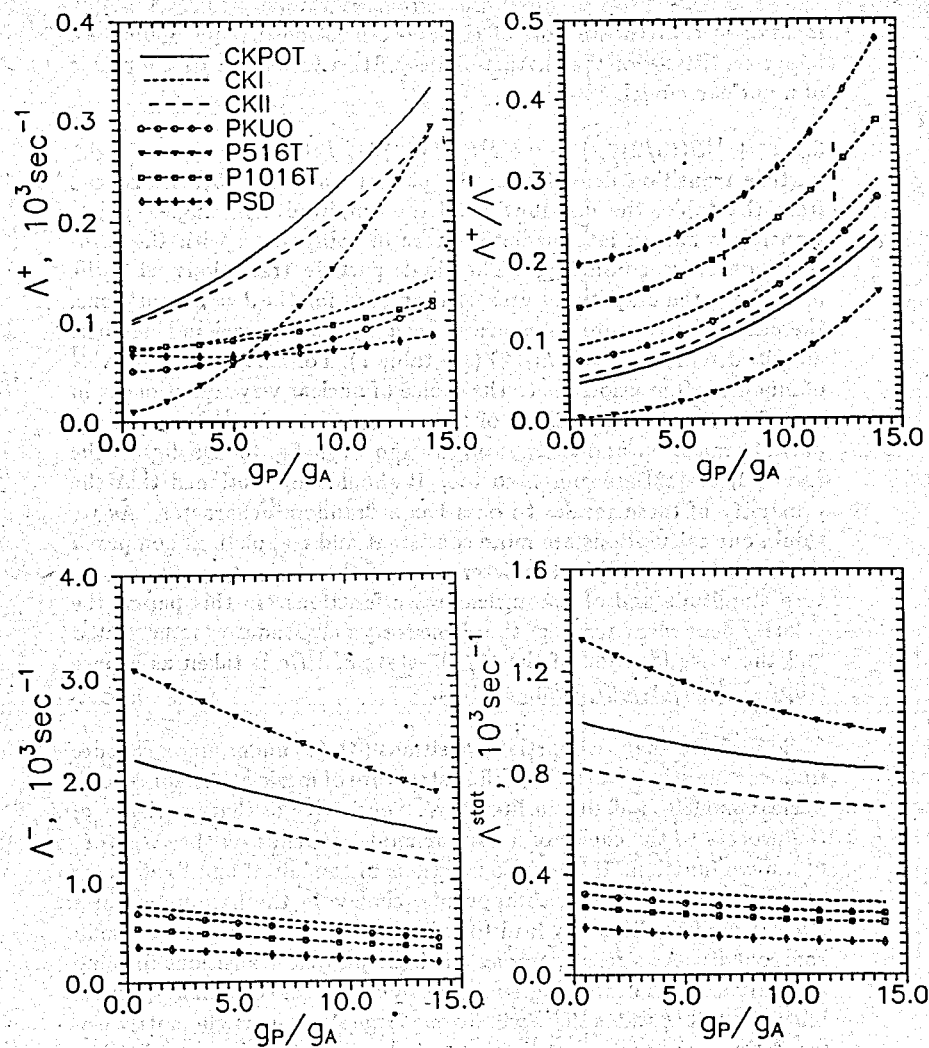


Fig. 2. Ordinary muon capture rates for partial transition $\mu^- + {}^{10}\text{B}(3_{g.s.}^+) \rightarrow \nu + {}^{10}\text{Be}(2_1^+, 3.37)$. The ratios Λ^+/Λ^- of [6] (table IV) are denoted by vertical bars. The rates Λ^+ , Λ^- and Λ^{stat} are too large to be placed on the figure

mentioned that the authors of the above-mentioned paper indicate a larger sensitivity of the characteristics of this transition to the choice of a nuclear model.

6. $\mu^- + {}^{11}\text{B}((3/2)_{g.s.}^-) \rightarrow \nu + {}^{11}\text{Be}((1/2)_1^-)$. Table 6 illustrates single-particle transition densities for the partial transition (5). As is seen from the table, the distribution of the amplitudes of single-particle transitions has an intermediate nature in comparison with the transition densities considered. The single-particle transitions with the $J = 1$ have the amplitudes greater than ones for the $J = 2$ transitions, therefore, the capture rates are defined by the allowed independent amplitudes $M_1(-1)$ and $M_1(2)$ (see table 7). For this case, sensitivity of muon capture velocities to the choice of nuclear wave functions is in the 15 per cent range. Rates of the muon capture by ${}^{11}\text{B}$ for a given partial transition and their ratio are shown in fig. 3. On fig 3. the results from [13] are presented too. It should be mentioned that the proximity of these results to ours has a "random" character. As we think, our calculations are more consistent and complete as compared to the results of [13] in the description of the elementary muon capture amplitude and of the nuclear wave functions. In this paper, the velocity dependent terms of the elementary amplitudes were neglected and the wave function of the $(1/2)_1^-$ -state of ${}^{11}\text{Be}$ is taken as a pure $((0p_{3/2})_{0,1}^6(0p_{1/2})_{1,2,3/2})$ configuration.

7. So we have analysed partial transitions (4)–(5) under muon capture from certain states of the hyperfine structure of mesic atoms for several nuclear models available in literature. Sensitivity of characteristics of the process to the choice of a nuclear model depends on the structure of a wave function. If the wave functions of the initial and final states contain manifest leading components, change in the parameters of a nuclear model will mainly lead to redistribution of amplitudes of small components. As a result, among all single-particle transitions forming a matrix element of the single-particle operator between many-particle initial and final states there will be one large single-particle matrix element giving the main contribution to independent nuclear amplitudes. In a situation like that a possible error in calculations of rates of muon capture which may be caused by uncertainty in the choice of nuclear wave functions is minimal. An example of that type of a process, favourable from the point of view of reliability of calculation, is the

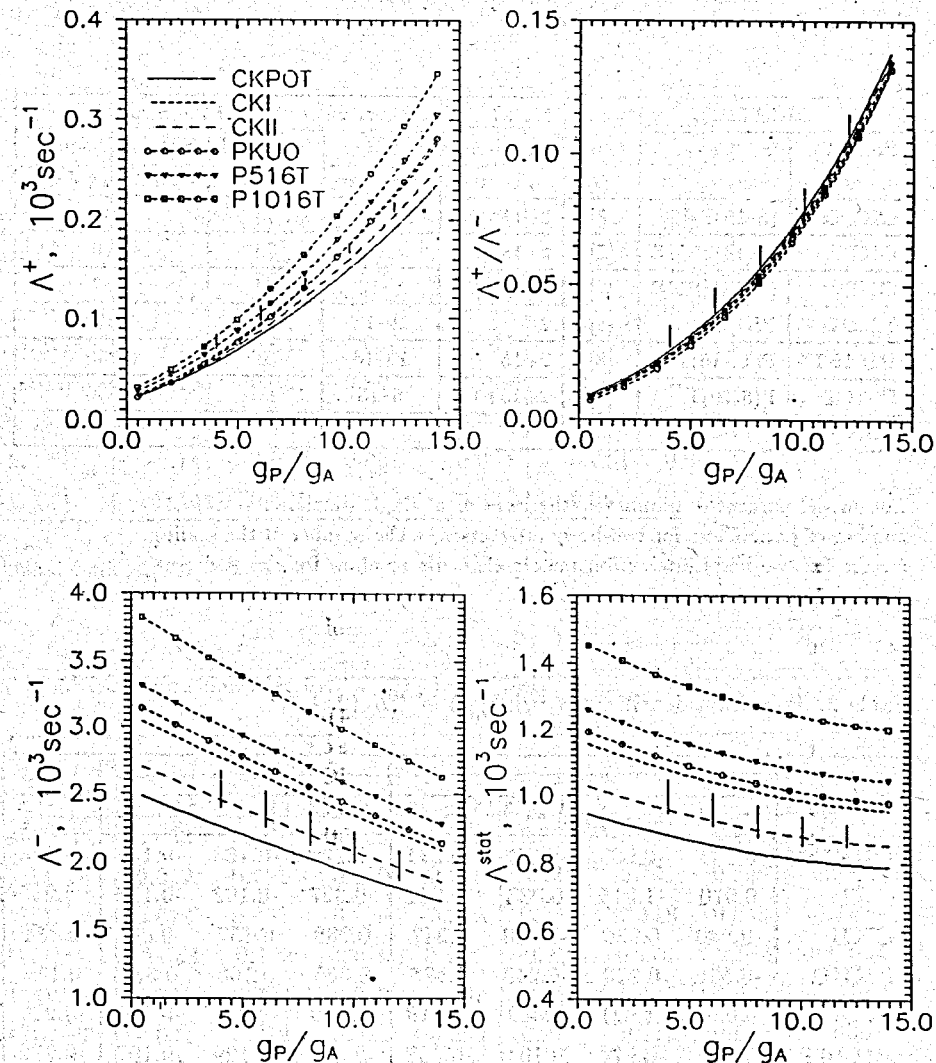


Fig. 3 Ordinary muon capture rates for partial transition $\mu^- + {}^{11}\text{B}((3/2)_{g.s.}^-) \rightarrow \nu + {}^{10}\text{Be}((1/2)_1^-)$, 0.320). The results of [13] are denoted by vertical bars. (The data are taken from tables I–III of [13])

Table 1. The used nuclear models

The model labels		Reference	Model parameter number	Short description of the fit procedure		
Present paper	in reference			A from - to	The level number	The mean square deviation (MeV)
CKPOT	(8-16)POT	[7]	2+11	8-16	35	0.43
CKI	(8-16)2BME	[7]	2+15	8-16	35	0.40
CKII	(6-16)2BME	[7]	2+15	6-16	44	0.57
PKUO	PKUO	[8]	2	10-16	51	1.312
P1016T	P(10-16)T	[8]	2+15	10-16	51	0.330
P516T	P(5-16)T	[8]	2+15+1	5-16	86	0.576
PSD		[9]				

The model parameter number = the number of single particle levels + the number of parameters for two-body interaction + the number of the scaling factors for two-body interaction matrix elements to allow for the A dependence.

Table 2. Transition densities for $^{10}B(3_{g.s.}^+) \rightarrow ^{10}Be(2_2^+)$

	J = 1				J = 2			J = 3
	$\frac{1}{2} \rightarrow \frac{1}{2}$	$\frac{3}{2} \rightarrow \frac{1}{2}$	$\frac{1}{2} \rightarrow \frac{3}{2}$	$\frac{3}{2} \rightarrow \frac{3}{2}$	$\frac{3}{2} \rightarrow \frac{1}{2}$	$\frac{1}{2} \rightarrow \frac{3}{2}$	$\frac{3}{2} \rightarrow \frac{3}{2}$	$\frac{3}{2} \rightarrow \frac{3}{2}$
CKPOT	0.044	-0.920	-0.012	-0.371	-0.278	-0.168	-0.155	-0.483
CKI	0.070	-1.015	0.083	-0.241	-0.327	-0.109	-0.113	-0.252
CKII	-0.040	0.936	-0.010	0.347	0.288	0.157	-0.097	0.434
PKUO	-0.076	0.933	-0.240	0.085	0.355	0.108	0.336	0.130
P516T	0.034	-1.031	0.069	-0.210	-0.320	-0.125	-0.124	-0.222
P1016T	0.034	-0.974	0.104	-0.282	-0.354	-0.129	-0.107	-0.272
PSD	-0.031	0.988	-0.134	0.182	0.309	0.121	0.210	0.152

Table 3. Independent amplitudes for $^{10}B(3_{g.s.}^+) \rightarrow ^{10}Be(2_2^+)$, ($g_P/g_A = 7.5$)

	J = 1		J = 2		J = 3	
	$M_1(-1)$	$M_1(2)$	$M_2(2)$	$M_2(-3)$	$M_3(-3)$	$M_3(4)$
CKPOT	-0.143	-0.046	-0.008	-0.003	0.011	0.003
CKI	-0.148	-0.048	-0.006	0.004	0.006	0.002
CKII	0.144	0.046	0.007	-0.003	-0.010	-0.003
PKUO	0.137	0.044	0.006	-0.006	-0.003	-0.001
P516T	-0.143	-0.047	-0.006	0.004	0.005	0.002
P1016T	-0.150	-0.048	-0.007	0.004	0.006	0.002
PSD	0.146	0.048	0.006	-0.005	-0.004	-0.001
-1.2 ^{a)}	-0.141	-0.045	-0.007	0.004	0.058	0.015
-1.4 ^{a)}	-0.144	-0.045	-0.006	0.004	0.061	0.016

^{a)} cited from [12], table 2.19.

Table 4. Transition densities for $^{10}B(3_{g.s.}^+) \rightarrow ^{10}Be(2_1^+)$

	J = 1				J = 2			J = 3
	$\frac{1}{2} \rightarrow \frac{1}{2}$	$\frac{3}{2} \rightarrow \frac{1}{2}$	$\frac{1}{2} \rightarrow \frac{3}{2}$	$\frac{3}{2} \rightarrow \frac{3}{2}$	$\frac{3}{2} \rightarrow \frac{1}{2}$	$\frac{1}{2} \rightarrow \frac{3}{2}$	$\frac{3}{2} \rightarrow \frac{3}{2}$	$\frac{3}{2} \rightarrow \frac{3}{2}$
CKPOT	0.033	0.521	-0.196	-0.191	0.334	-0.114	0.624	-0.759
CKI	0.012	0.281	-0.220	-0.228	0.239	-0.191	0.609	-0.882
CKII	0.023	0.492	-0.200	-0.218	0.299	-0.118	0.643	-0.772
PKUO	-0.018	-0.182	0.153	0.116	-0.219	0.276	-0.514	0.931
P516T	0.051	0.229	-0.240	-0.267	0.261	-0.180	0.669	-0.944
P1016T	0.034	0.299	-0.176	-0.260	0.274	-0.212	0.668	-0.900
PSD	0.058	0.125	-0.196	-0.308	0.211	-0.191	0.659	-0.909

Table 5. Independent amplitudes for $^{10}B(3_{g.s.}^+) \rightarrow ^{10}Be(2_1^+)$,
($g_p/g_A = 7.5$)

	J = 1		J = 2		J = 3	
	$M_1(-1)$	$M_1(2)$	$M_2(2)$	$M_2(-3)$	$M_3(-3)$	$M_3(4)$
CKPOT	0.051	0.019	0.002	-0.004	0.018	0.006
CKI	0.025	0.009	0.000	-0.002	0.021	0.007
CKII	0.045	0.017	0.001	-0.004	0.018	0.006
PKUO	-0.021	-0.007	0.001	-0.001	-0.022	-0.007
P516T	0.062	0.015	-0.002	-0.004	-0.004	0.000
P1016T	0.017	0.008	-0.000	-0.002	0.021	0.007
PSD	-0.005	0.000	-0.001	-0.002	0.022	0.007
-1.2 ^{a)}	0.025	0.009	0.0	-0.003	0.076	0.020
-1.4 ^{a)}	0.034	0.012	0.0	-0.003	0.081	0.021

^{a)} cited from [12], table 2.19.

Table 6. Transition densities for $^{11}Be(\frac{3}{2}^-) \rightarrow ^{11}Be(\frac{1}{2}^-)$

	J = 1				J = 2		
	$\frac{1}{2} \rightarrow \frac{1}{2}$	$\frac{3}{2} \rightarrow \frac{1}{2}$	$\frac{1}{2} \rightarrow \frac{3}{2}$	$\frac{3}{2} \rightarrow \frac{3}{2}$	$\frac{3}{2} \rightarrow \frac{1}{2}$	$\frac{1}{2} \rightarrow \frac{3}{2}$	$\frac{3}{2} \rightarrow \frac{3}{2}$
CKPOT	-0.019	-0.606	-0.340	-0.179	-0.63	0.075	0.088
CKI	0.016	0.5998	0.330	0.215	0.652	-0.068	-0.119
CKII	-0.016	-0.602	-0.344	-0.201	-0.637	0.077	0.103
PKUO	0.006	0.571	0.366	0.276	0.636	-0.062	-0.140
P516T	0.018	0.640	0.336	0.206	0.637	-0.031	-0.087
P1016T	0.016	0.657	0.285	0.179	0.695	-0.044	-0.072

Table 7. Independent amplitudes for $^{11}Be(\frac{3}{2}^-) \rightarrow ^{11}Be(\frac{1}{2}^-)$,
($g_p/g_A = 7.5$)

	J = 1		J = 2	
	$M_1(-1)$	$M_1(2)$	$M_2(2)$	$M_2(-3)$
CKPOT	-0.066	-0.026	-0.015	-0.000
CKI	0.073	0.028	0.016	-0.000
CKII	-0.069	-0.027	-0.015	0.000
PKUO	0.075	0.028	0.016	-0.000
P516T	0.077	0.029	0.017	-0.002
P1016T	0.083	0.031	0.017	-0.000

transition $\mu^- + ^{10}B(3_{g.s.}^+) \rightarrow \nu + ^{10}Be(2_2^+)$. The rates Λ^+ , Λ^- and Λ^{stat} change within 8 ÷ 10 per cent when the nuclear model changes. But the ratio Λ^+/Λ^- varies within 2 ÷ 3 per cent at the same time being sensitive to the value of g_p . Analogously, in the case of ^{11}B ordinary muon capture the measured ratio Λ^+/Λ^- can be a source of precise information about g_p . Preliminary analysis of single-particle transition densities seems to be very useful in choosing a target nucleus and in preparing an experiment.

The present work was fulfilled at the Bogoliubov Theoretical Laboratory of JINR (Dubna) and PSI.

In conclusion, the authors express their gratitude for useful discussions and support to Prof. E. Boschitz (University of Karlsruhe), Prof. R. Prieels (Universite Catholique de Louvain), Prof. R.A. Er-amzhyan (IYal Russian Academy of Sciences) and to V.B. Brudanin, S.V. Egorov, S.N. Ershov and S.S. Kamalov (all from JINR).

References

- [1] Hasinoff M.D. et al. // TRI-PP-93-30, Vancouver, 1993
- [2] Morita M. and Fujii A. // Phys. Rev., 1960, **118**, 606
- [3] Balashov V.V. and Eramzhyan R.A. // Atomic Energy Review, 1967, **5**, 3, Vienna
- [4] Deutsch J., Grenacs L. et al. // PSI report R-92-04, PSI, 1992
- [5] Desgrolard P. and Guignon P.A.M. // Phys. Rev., 1979, **C19**, 120
- [6] Bukhvostov A.P. et al. // Acta Phys. Polonica, 1972, **B 3**, 375
- [7] Cohen S. and Kurath D. // Nucl. Phys., 1965, **73**, 1
- [8] Warburton E.K. and Brown B.A. // Phys. Rev. C, 1992, **46**, 923
- [9] Millener D.J. and Kurath D. // Nucl. Phys., 1975, **A255**, 315
- [10] Brown B.A. and Wildenthal B.H. // At. Data and Nucl. Data Tables, 1985, **33**, 347
- [11] Etchegoyen A., Brown B.A., Rae W.D.M. // MSUCL Report Number 524, Michigan, 1984
- [12] Balashov V.V., Korenman G.Ya. and Eramzhyan R.A., The mesons capture by atomic nuclei, M., Atomizdat, 1978 (in Russian)
- [13] Bernabeu J. // Nuovo Cim., 1971, **4 A**, 715

Received by Publishing Department
on October 8, 1993.